

Maternal Rnf12/RLIM is required for imprinted X-chromosome inactivation in mice

JongDae Shin¹, Michael Bossenz^{5*†}, Young Chung^{6,7*}, Hong Ma¹, Meg Byron⁴, Naoko Taniguchi-Ishigaki¹, Xiaochun Zhu^{1,3}, Baowei Jiao¹, Lisa L. Hall⁴, Michael R. Green^{1,2,3}, Stephen N. Jones⁴, Irm Hermans-Borgmeyer⁵, Jeanne B. Lawrence⁴ & Ingolf Bach^{1,2}

Two forms of X-chromosome inactivation (XCI) ensure the selective silencing of female sex chromosomes during mouse embryogenesis. Imprinted XCI begins with the detection of *Xist* RNA expression on the paternal X chromosome (Xp) at about the four-cell stage of embryonic development. In the embryonic tissues of the inner cell mass, a random form of XCI occurs in blastocysts that inactivates either Xp or the maternal X chromosome (Xm)^{1,2}. Both forms of XCI require the non-coding *Xist* RNA that coats the inactive X chromosome from which it is expressed. *Xist* has crucial functions in the silencing of X-linked genes, including *Rnf12* (refs 3, 4) encoding the ubiquitin ligase RLIM (RING finger LIM-domain-interacting protein). Here we show, by targeting a conditional knockout of *Rnf12* to oocytes where RLIM accumulates to high levels, that the maternal transmission of the mutant X chromosome (Δ m) leads to lethality in female embryos as a result of defective imprinted XCI. We provide evidence that in Δ m female embryos the initial formation of *Xist* clouds and Xp silencing are inhibited. In contrast, embryonic stem cells lacking RLIM are able to form *Xist* clouds and silence at least some X-linked genes during random XCI. These results assign

crucial functions to the maternal deposit of Rnf12/RLIM for the initiation of imprinted XCI.

RLIM is a ubiquitin ligase that regulates the activity of various transcription factors and cofactors^{5–8}. It is encoded by the *Rnf12* gene⁹, which is located about 500 kilobases (kb) telomeric to the *Xist* gene on the X chromosome. During mouse embryogenesis, RLIM protein and its messenger RNA are ubiquitously expressed at embryonic day (E)7.5/E8.0 (refs 5, 10), in pre-implantation embryos at E3.5 (Supplementary Fig. 1), and in mouse embryonic stem (ES) cells (Supplementary Fig. 2). In ovaries, we detected particularly high levels of RLIM in oocytes, oocyte-supporting granulosa cells and follicle-surrounding theca cells (Fig. 1a). RLIM levels in pronuclei were high at all stages of oocyte differentiation in 10-week-old and 5-week-old mice (Fig. 1a, b). As oocytes in 5-week-old females are immature, these results indicate that RLIM accumulates during oocyte maturation.

To generate a mouse model carrying a conditional *Rnf12* allele we flanked the coding region of exon 5 with *loxP* sites (Supplementary Fig. 2). Exon 5 encodes 517 of RLIM's total of 600 amino-acid residues⁹ including the RING finger. We targeted the *Rnf12* knockout (Δ) to

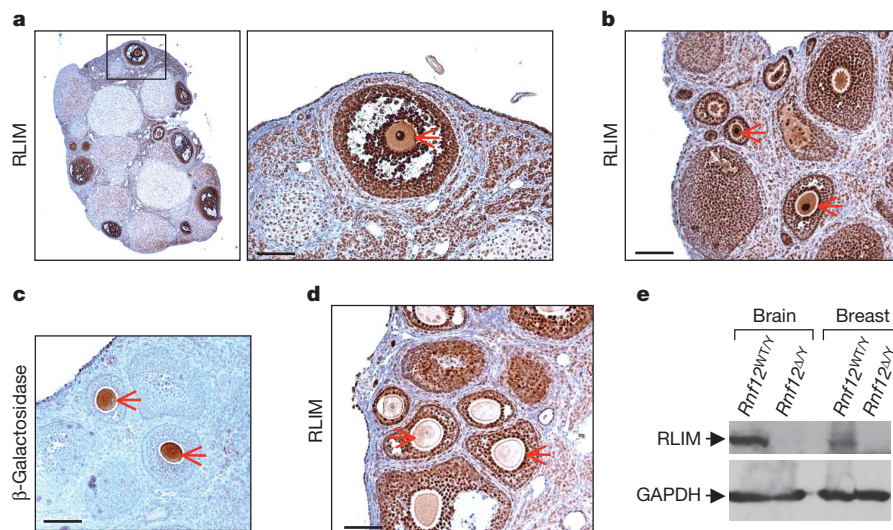


Figure 1 | RLIM accumulates during oocyte maturation. **a**, Ovary sections from a 10-week-old *fl/fl* female, stained immunohistochemically with anti-RLIM antibodies. Right: higher magnification of boxed region. **b**, RLIM staining of ovaries from 5-week-old *fl/fl* animals. **c**, MMTV-LTR-induced Cre expression in oocytes. The *Rosa26 loxP-stop-loxP-lacZ* reporter strain mouse (R26R) was crossed to *MMTV-Cre* (line F) mice. Paraffin-embedded sections of ovaries of 5-week-old females were stained with antibodies against β -galactosidase. **d**, Ovarian section of a 10-week-old *Rnf12^{fl/fl} × MMTV-Cre*

female stained with anti-RLIM antibodies. Note the loss of RLIM detection in oocytes but not in surrounding granulosa cells. Oocytes are indicated by red arrows in **a–d**. **e**, Knockout of the *Rnf12* gene leads to a loss of RLIM protein in mice. Top: western blot analysis of protein extracts prepared from brain and breast tissues of WT and *Rnf12* knockout male mice (WT/Y and Δ /Y, respectively) stained with anti-RLIM antibodies. Bottom: as control, the same blot was probed with antibodies against glyceraldehyde-3-phosphate dehydrogenase (GAPDH). Scale bars, 80 μ m.

¹Program in Gene Function and Expression, University of Massachusetts Medical School (UMMS), Worcester, Massachusetts 01605, USA. ²Program in Molecular Medicine, UMMS, Worcester, Massachusetts 01605, USA. ³Howard Hughes Medical Institute, UMMS, Worcester, Massachusetts 01605, USA. ⁴Department of Cell Biology, UMMS, Worcester, Massachusetts 01605, USA. ⁵Centre for Molecular Neurobiology, University of Hamburg, 20246 Hamburg, Germany. ⁶Stem Cell and Regenerative Medicine International, Inc., Marlborough, Massachusetts 01752, USA. ⁷CHA University, School of Medicine, Seoul 135-081, Korea. [†]Present address: Institute for Biochemistry and Cell Biology, University of Magdeburg, 39120 Magdeburg, Germany.

*These authors contributed equally to this work.

oocytes by using transgenic mice that express Cre recombinase (Cre) under the control of the mouse mammary tumour virus long terminal repeat (MMTV-LTR). Several *MMTV-Cre* mouse lines exist, some of which target the female germ line¹¹. Cre expression in oocytes was verified by crossing *MMTV-Cre* (line F) mice to *Rosa26-loxP-stop-loxP-lacZ* animals¹² (Fig. 1c). Ovaries from *Rnf12^{fl/fl}* × *MMTV-Cre* (line F) females (*fl/fl-Cre*) showed a lack of RLIM in oocytes but not in the surrounding granulosa cells or in stromal cells (Fig. 1d), confirming a *Rnf12* knockout in oocytes. The correct targeting was corroborated by the fact that we obtained knockout males with a germline deletion of the *Rnf12* gene (Δ/Y), lacking RLIM in all somatic tissues examined (Fig. 1e, and not shown). Because Δ/Y males are viable and fertile, these results demonstrate that *Rnf12*/RLIM is not required for basic cellular or developmental functions, for the maturation of oocytes or for meiotic sex-chromosome inactivation.

Pups born to *fl/fl* females showed normal sex ratios, and a normal transmission of the paternal X chromosomes (p) was observed in matings with wild-type (WT), *fl* or Δp males (Fig. 2a, mating schemes 1–3). However, no female offspring carrying a maternally transmitted knockout (Δm) allele was born to *fl/fl-Cre* or *WT/fl-Cre* females crossed with WT, *fl* or Δp males (Fig. 2a, schemes 4 and 5, and not

shown), whereas the Δm allele was transmitted efficiently to male pups. The probability of obtaining male versus female pups from *fl/fl-Cre* or *WT/fl-Cre* females was highly significant ($P < 2 \times 10^{-8}$). In contrast, *WT/fl-Cre* females transmitted the WT allele normally, and the probabilities of producing male WT/Y versus male *fl/Y* or $\Delta m/Y$ offspring were similar ($P > 0.13$) (Fig. 2a, mating scheme 5). We also performed matings with the *MMTV-Cre* line D, which does not target to the female germ line¹¹, and observed normal Mendelian distributions for male and female pups ($n = 177$; not shown) born to *fl/fl-Cre* (line D) females. These findings, together with a decreased mean litter size for matings 4 and 5, indicated that the deletion of *Rnf12* in the maternal germ line leads to embryonic lethality. As mice were bred in a congenic C57BL/6 background to eliminate strain-specific influences, our results reveal a sex-specific parent-of-origin effect.

Next, we examined embryos that received either a Δm or a Δp allele. Whereas male $\Delta m/Y$ embryos had a normal appearance, the maternal transmission of the knockout allele to female conceptuses in the same litters resulted in severe growth defects that were apparent as early as E7.5 (Fig. 2b–e). However, generating this heterozygous genotype with paternal transmission of the knockout allele resulted in female *fl/\Delta p* embryos with a normal appearance (Fig. 2f). Embryonic components of Δm conceptuses differed in size and showed various degrees of disorganization (Fig. 2g, h). The embryo shown in Fig. 2g was the largest observed female Δm embryo. No obvious differences in severity of growth defects between heterozygous $\Delta m/fl$ and Δ/Δ female embryos were detected at E7.5, E8.5 or E9.5 (Fig. 2 and Supplementary Fig. 3a–c). We were unable to recover Δm female conceptuses at stages later than E11.5, presumably as a result of reabsorption. Quantifications of phenotypes showed that all recovered Δm female embryos had growth defects (Supplementary Fig. 3d). In 25% of deciduals we were unable to recover a conceptus. As this corresponds to the number of missing female embryos expected for a Mendelian ratio it is highly likely that these corresponded to Δm females.

On examination of Δm blastocyst outgrowths at pre-implantation stages, trophoblast migration, cell number and expression of the early trophoblast marker Troma-1 (ref. 13) seemed comparable to those of controls (Supplementary Fig. 4a, b). For analyses at early post-implantation stages we sectioned through entire E5.5 and E6.5 deciduas born of a *fl/\Delta-Cre* × Δ/Y cross. From this mating, about 50% of the embryos should correspond to Δm females. Indeed, haematoxylin/eosin (H&E) stainings revealed about 50% of mildly or severely disorganized embryos (Supplementary Fig. 4c, d). These results suggest that growth defects in Δm embryos first occur at about the time of implantation or very shortly thereafter. Next, we examined the effects of the *Rnf12* knockout on the development of extraembryonic tissues and analysed placentae of Δm embryos in the cases when a conceptus was found. H&E stainings revealed that most, if not all, tissues derived from the extraembryonic trophoblast were missing in $\Delta m/fl$ placentae at E10.5 ($n = 4$) and E9.5 ($n = 5$), whereas the maternal deciduas had a normal appearance (Supplementary Fig. 5a, b). This was accompanied by a lack of the trophoblast markers PAI-1 (plasminogen activator inhibitor type 1) and *Cdx2* (refs 14, 15) as early as E8.5 during placental development ($n = 4$) (Supplementary Fig. 5c; not shown). Because these phenotypes are reminiscent of those described for female *Xist* knockout embryos caused by a paternally inherited *Xist* knockout allele¹⁶, we speculated that *Rnf12* might regulate XCI.

We first examined random XCI in *WT/\Delta p* adult females and found that almost all somatic cells in ovaries of *WT/\Delta p* adult females ($n = 3$) stained positive for RLIM (Supplementary Fig. 6a), and general RLIM levels in somatic tissues were similar in *WT/\Delta p* and *WT* adult females (Supplementary Fig. 6b). Because the ratio of *fl/\Delta p* female to male Δ/Y pups (Fig. 2a, scheme 3) was normal, these results suggest that in *WT/\Delta p* adult females random XCI is skewed towards the mutated allele. Staining mouse embryonic fibroblasts (MEFs) of *fl/\Delta p* embryos at E12.5 with antibodies against RLIM and histone 3 tri-methylated at Lys 27 (H3K27me3)¹⁷ revealed that 94% ($n = 300$ of three embryos) of

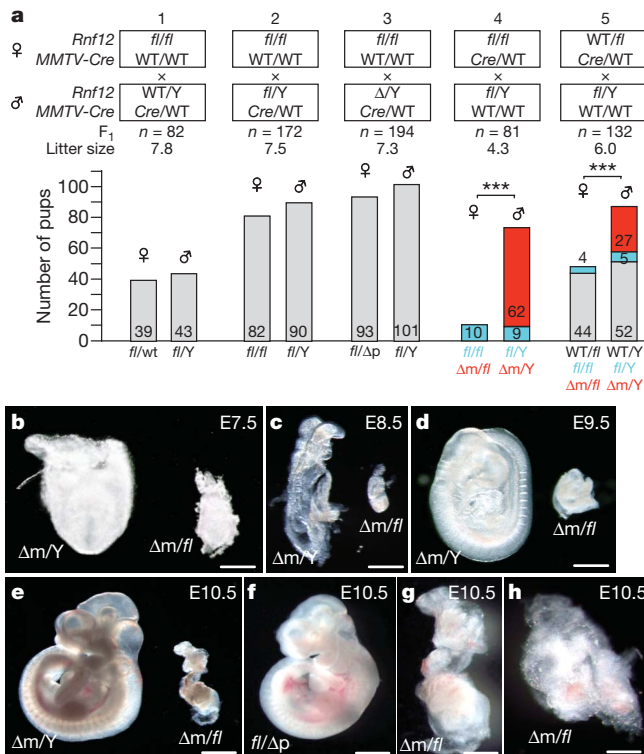


Figure 2 | A maternally transmitted *Rnf12* deletion allele leads to early embryonic lethality specifically in females. **a**, *MMTV-Cre*-mediated loss of Δm females. Schematic diagram of born pups from the indicated mating schemes (1–5). Parental genotypes of female (upper) and male (lower) mice with respect to *Rnf12* and *MMTV-Cre* are shown and the total number (n) of F_1 offspring and the mean litter size are indicated. The numbers of offspring (grouped into females and males) and their genotypes with respect to *Rnf12* are indicated on the x axis and y axis, respectively. m (maternal) and p (paternal) indicate the origin of the knockout (Δ) allele. In mating schemes 4 and 5, maternally transmitted WT, floxed and Δ alleles are indicated in grey, blue and red, respectively. Three asterisks, $P < 10^{-7}$. **b–e**, Heterozygote $\Delta m/fl$ female and homozygote $\Delta m/Y$ littermates from a *fl/\Delta p* × *fl/Y* cross at E7.5 (**b**); E8.5 (**c**); E9.5 (**d**) and E10.5 (**e**). **f**, Heterozygote *fl/\Delta p* female at E10.5 from a *fl/fl* × Δ/Y cross. **g**, Best-developed $\Delta m/fl$ embryo ($n = 28$) detected at E10.5 (magnification of the $\Delta m/fl$ embryo shown in **e**). **h**, Representative Δm female embryo at E10.5. Scale bars, 0.15 mm (**b**); 0.4 mm (**c**); 0.6 mm (**d**); 1 mm (**e**, **f**); 0.5 mm (**g**); 0.25 mm (**h**). In **b–h** embryos were first photographed and then processed for genotyping.

MEFs stained positive for RLIM and H3K27me3 (Fig. 3a). In addition, in RNA fluorescence *in situ* hybridization (FISH) experiments using a double-stranded *Xist* probe that recognizes *Xist* and *Tsix* showed that 97% ($n = 300$ of three embryos) of the stained MEFs showed specific *Xist* points on one X chromosome.

To test the status of the *Rnf12* gene on the inactive X chromosome, we performed RNA FISH with probes against *Xist* and *Rnf12*. For *Rnf12* we used a 12-kb genomic probe located 5' of the deletion site that recognizes WT and Δ transcripts of the *Rnf12* gene equally well (Supplementary Fig. 7b). Results revealed that 92% of MEFs that expressed *Xist* also expressed *Rnf12* in a monoallelic fashion similar to *fl/fl* control MEFs (Fig. 3b). Next, we generated ES cells lacking *Rnf12* and isolated the heterozygous *fl/ Δ p* line 7 and Δ/Δ ES lines 4, 6, 11 and 23 (Supplementary Fig. 7a; not shown). Consistent with skewed random XCI was our finding that 98% of H3K27me3-positive embryoid-body-differentiated *fl/ Δ p* line 7 ES cells expressed RLIM protein, whereas Δ/Δ ES cells did not (Supplementary Fig. 7c, not shown). All Δ/Δ ES lines stained positive for H3K27me3 and developed *Xist* clouds on differentiation (Fig. 3c, d, and data not shown). A time course comparing WT female ES cells with *fl/ Δ p* line 7, Δ/Δ line 4 and Δ/Δ line 23 revealed a slower initiation of XCI at days 2 and 4 during embryoid body differentiation (Fig. 3c). However, at days 6 and 8 these differences were no longer significant. The rates of *Xist* cloud formation of Δ/Δ and *fl/ Δ p* ES cells were similar ($P > 0.05$). To assess X silencing in mutant ES cells we hybridized cells with both *Xist* and *Rnf12* probes in RNA FISH at 2, 4, 6 and 8 days of embryoid body differentiation. Focusing on cells with *Xist* clouds (set to 100%) we compared the distribution of *Rnf12* signals in nuclei showing either monoallelism, biallelic or no signal. Silencing of the *Rnf12* gene was slower in all *Rnf12* mutant ES cells at 2, 4 and 6 days of differentiation in comparison with WT cells ($P < 0.05$). Again, mutated ES cells did not differ significantly between themselves (Fig. 3d). Silencing of *Pgk1*,

another X-linked gene, was also observed in *Rnf12* mutant ES cells after 6 days of embryoid body differentiation (Supplementary Fig. 7d). These results, combined with our finding that in teratoma assays, in which ES cells are injected into kidney capsules of immunodeficient NOD-SCID mice, Δ/Δ cells participate in the formation of ectodermal, endodermal and mesodermal germ layers and derived cell types (Supplementary Fig. 7e), indicate that ES cells lacking RLIM/*Rnf12* initiate XCI. Our data also suggest that random XCI is skewed towards the mutated *Rnf12* allele in *fl/ Δ p* females.

Because these results did not explain the observed embryonic lethality (Fig. 2), we next investigated imprinted XCI in E3.5 and E4.5 blastocyst outgrowths by means of RNA FISH. When required, embryo gender was determined by isolation of the inner cell mass (ICM) after image recording and genotyping for the presence of the *Zfy* gene and, as control, the β -actin gene by PCR. A high percentage of central cells in the ICM of control and Δ m E4.5 blastocyst outgrowths developed *Xist* clouds or single pinpoints, indicating transcription foci (Fig. 4a, Supplementary Movies 1 and 2 and Supplementary Fig. 8a). This suggests that, in contrast with ES cells in culture, random XCI occurs with similar kinetics in blastocysts. However, although quantification of ICM stainings was not possible because of a high cell density, the smaller number of E4.5 ICM cells staining positive for H3K27me3 (ref. 17) in Δ m in comparison with WT blastocysts (Supplementary Fig. 8b) suggested that imprinted XCI is inhibited in primitive endoderm cells. Focusing on trophoblasts that also undergo imprinted XCI, only about 10% of Δ/Δ and Δ m cells displayed *Xist* clouds, in contrast with more than 90% of *fl/fl* and *fl/ Δ p* cells (Supplementary Fig. 9a–d). Higher magnification revealed the presence of pinpoints in about 20% of Δ m trophoblasts at E4.5, and 30% at E3.5. Generally one pinpoint per trophoblast was detected although some cells developed two pinpoints, probably as a result of the development of polyploidism¹⁸. The parental origin of these *Xist* signals was not examined and because we used a double-stranded

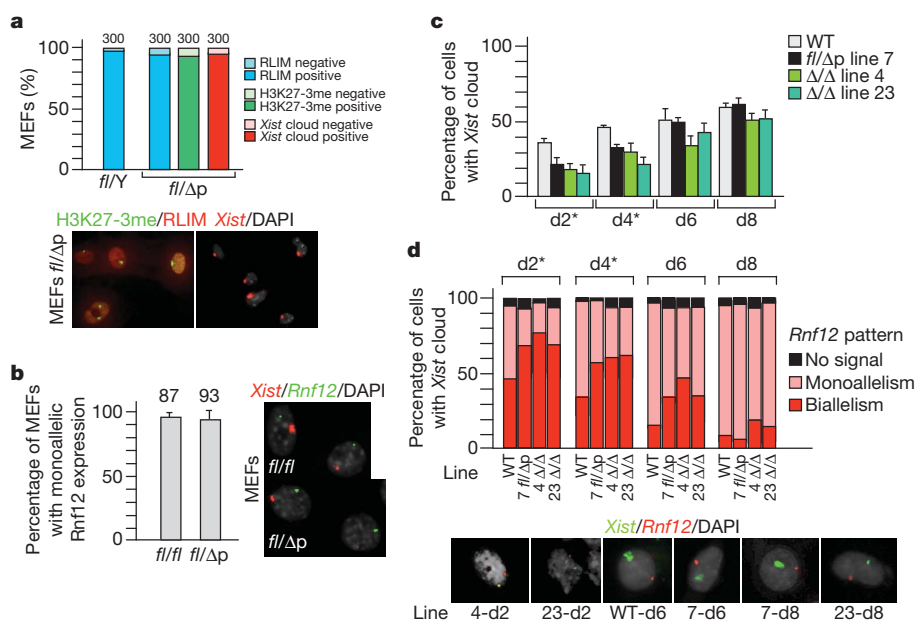


Figure 3 | *Rnf12* is not required for initiation of random XCI. **a**, MEFs of E12.5 *fl/ Δ p* and *fl/Y* males were stained simultaneously with antibodies against RLIM and H3K27me3 or with a *Xist* probe using RNA FISH. Top: summary graph representing three independent experiments. Error bars represent s.d. Cells were scored for RLIM expression, the presence of H3K27me3 staining or *Xist* clouds. Bottom left: representative image with RLIM (red) and H3K27me3 (green) staining. Bottom right: representative image of *Xist* staining (red). DAPI, 4',6-diamidino-2-phenylindole. **b**, Left: summary graph of RNA FISH experiments on E12.5 *fl/ Δ p* MEFs stained simultaneously with probes against *Xist* and *Rnf12*. Left: representative images showing monoallelic expression. Numbers above the bars in **a** and **b** are the numbers of cells. **c**, **d**, Time courses

of initiation of XCI (**c**) and silencing of *Rnf12* (**d**) in ES cell lines. ES cells were embryoid-body-differentiated for the indicated duration in days (d) before simultaneous staining with RNA FISH, using *Xist* and *Rnf12* probes.

c, Percentage of *Xist*-positive ES cells. Error bars represent s.d. Asterisks indicate significant differences between the wild type and each of the three Δ cell lines ($P < 0.05$). **d**, *Xist*-positive cells were scored for monoallelic or biallelic *Rnf12* expression, or no signal. Top: summary graph. Bottom: representative images of various ES cells with biallelic and monoallelic *Rnf12* expression. Asterisks indicate significant differences between WT and each of the three Δ cell lines ($P < 0.05$).

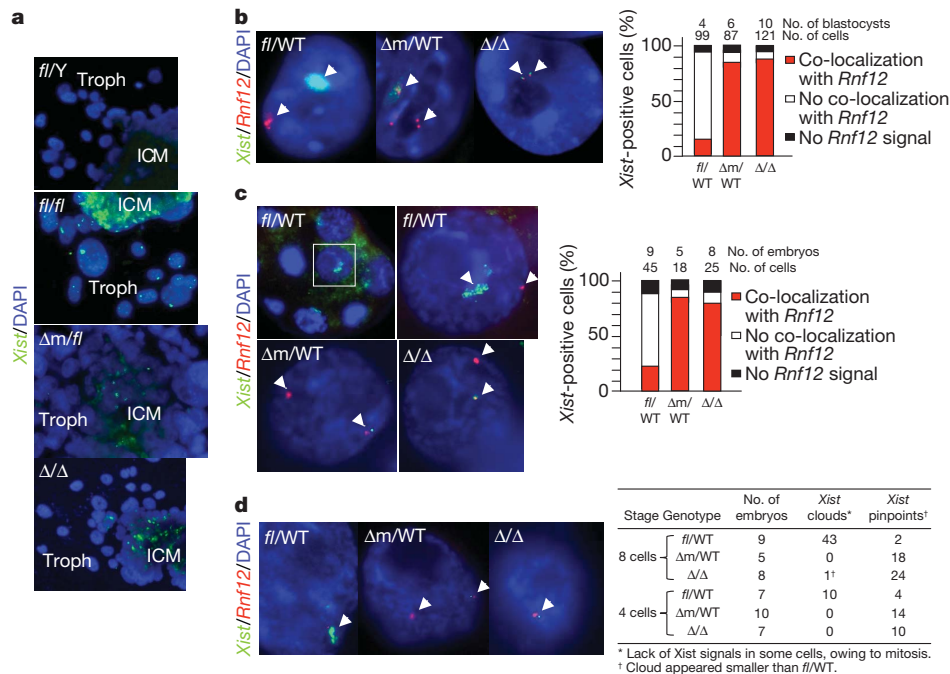


Figure 4 | Regulation of *Xist* cloud formation and X silencing by *Rnf12* during imprinted XCI. Probes for RNA FISH were *Xist* (green) and *Rnf12* (red). **a**, Representative E4.5 blastocyst outgrowths stained with *Xist*. Troph, trophoblasts. **b**, Representative E3.5 trophoblasts from *fl/WT*, $\Delta m/WT$ and Δ/Δ mice, stained with *Xist* and *Rnf12*. Right: for quantification, *Xist*-positive trophoblasts (clouds or pinpoints) were scored for co-localization with

Xist probe we cannot distinguish between *Xist* and *Tsix* pinpoints. Co-stainings with antibodies directed against RLIM and H3K27me3 revealed that only about 10% of Δ/Δ trophoblasts showed H3K27me3 signals, compared with 94% in *fl/fl* trophoblasts (Supplementary Fig. 10a–c). To compare *Xist* expression in blastocysts quantitatively and to monitor the expression of *Tsix*^{2,19,20}, we performed reverse-transcriptase-mediated quantitative PCR (RT–qPCR) on E3.5 and E4.5 blastocysts, comparing Δ/Δ with *fl/fl* embryos (Supplementary Fig. 11a). In agreement with results obtained by RNA FISH, *Xist* expression was decreased in Δ/Δ females. *Tsix* levels were only mildly affected in E3.5 embryos and were lower at E4.5, suggesting that RLIM does not induce *Xist* by repression of *Tsix* RNA transcription. Increased *Pgk1* levels suggested defects at the level of Xp silencing.

To investigate Xp silencing we co-hybridized E3.5 blastocyst outgrowths with the *Xist* probe and with probes recognizing the X-linked genes *Pgk1* or *Rnf12*. Although both *Pgk1* and *Rnf12* were efficiently silenced on Xp in control trophoblasts, we observed at least two spots of *Pgk1* or *Rnf12* in a high percentage of Δm trophoblasts, with at least one signal in proximity of a *Xist* pinpoint (Fig. 4b and Supplementary Fig. 11b, c). Furthermore, the formation of nuclear compartments around Xp that exclude Cot-1 RNA or general transcription factors such as TATA-box-binding protein (TBP)^{21,22} was inhibited in Δm trophoblasts (Supplementary Fig. 12, and not shown). Defects in *Rnf12* silencing were observed as early as the eight-cell stage (Fig. 4c). Because this is the earliest stage at which X-linked genes are silenced^{3,4}, these results indicate that defects do not occur at the maintenance level. This is also in agreement with the finding that Δm cells did not form initial *Xist* clouds in eight-cell-stage or four-cell-stage embryos (Fig. 4c, d). However, because we detected one *Xist* transcription foci in a significant number of cells and *Xist* accumulation is regulated at the transcriptional level²³, our data are consistent with a crucial role for RLIM/Rnf12 for the transcriptional upregulation of *Xist*. The fact that a small but significant number of Δm trophoblasts developed *Xist* clouds (Supplementary Fig. 9) indicates that RLIM is not absolutely required for *Xist* upregulation but rather for it to occur reliably at the appropriate

time. Indeed, RLIM is able to modulate the transcriptional activity of various classes of transcription factors^{5,8}. While our manuscript was in preparation, a paper was published showing that overexpression of RLIM/Rnf12 initiates random XCI in ES cells²⁴. Although the reported data are in general agreement with our results, our finding that *Rnf12*^{−/−} ES cells initiate random XCI was surprising, suggesting the existence of several competence factors that may compensate for the lack of RLIM/Rnf12. Our *in vivo* data show that RLIM/Rnf12 is required for imprinted XCI, suggesting that it may be the only competence factor present in high concentrations during imprinted XCI. Indeed, the observed female parent-of-origin effect in XCI in Δm females (Fig. 2) suggests that the maternal deposit of RLIM/Rnf12 protein in oocytes drives imprinted XCI, and several observations support this view: first, RLIM protein or its mRNA accumulates to high levels in oocytes (Fig. 1); second, RLIM is undetectable in early two-cell-stage embryos carrying a Δm allele (Supplementary Fig. 13); third, overexpression of RLIM protein can initiate random XCI²⁴; fourth, the paternal contribution of RLIM/Rnf12 seems irrelevant for imprinted XCI (Fig. 2); and fifth, it explains why imprinted XCI occurs in *fl/Δp* females (Fig. 2 and Supplementary Fig. 9). Indeed, the maternal deposit of mRNA or protein to control early embryogenesis represents a mechanism that is widespread among many species²⁵ including mice²⁶. We therefore propose that maternal Rnf12/RLIM acts as a crucial regulator for the initiation of imprinted XCI in mice (Supplementary Fig. 14).

METHODS SUMMARY

Mice were generated in which the coding region of exon 5 of the *Rnf12* gene was flanked by *loxP* sites. Exon 5 was deleted in oocytes by means of *MMTV-Cre*. All embryos and blastocyst outgrowths examined were derived from natural matings. E3.5 or E4.5 blastocysts were cultured for 2–3 days on gelatin-coated coverslips as described²⁷. Immunocytochemistry and western blots were performed as reported²⁸. Paraffin-embedded sections of mouse tissues were stained with H&E (Histoserv, Inc.). Immunohistochemical stainings were performed in the Diabetes and Endocrinology Research Center Morphology Core at UMMS. Procedures

used for establishing mouse ES cells have been described²⁹. RNA FISH experiments were performed as reported²¹.

Full Methods and any associated references are available in the online version of the paper at www.nature.com/nature.

Received 17 March; accepted 26 August 2010.

1. Heard, E. & Disteche, C. M. Dosage compensation in mammals: fine-tuning the expression of the X chromosome. *Genes Dev.* **20**, 1848–1867 (2006).
2. Payer, B. & Lee, J. T. X chromosome dosage compensation: how mammals keep the balance. *Annu. Rev. Genet.* **42**, 733–772 (2008).
3. Patrat, C. *et al.* Dynamic changes in paternal X-chromosome activity during imprinted X-chromosome inactivation in mice. *Proc. Natl Acad. Sci. USA* **106**, 5198–5203 (2009).
4. Kalantry, S., Purushothaman, S., Bowen, R. B., Starmer, J. & Magnuson, T. Evidence of Xist RNA-independent initiation of mouse imprinted X-chromosome inactivation. *Nature* **460**, 647–651 (2009).
5. Bach, I. *et al.* RLIM inhibits functional activity of LIM homeodomain transcription factors via recruitment of the histone deacetylase complex. *Nature Genet.* **22**, 394–399 (1999).
6. Ostendorff, H. P. *et al.* Ubiquitination-dependent cofactor exchange on LIM homeodomain transcription factors. *Nature* **416**, 99–103 (2002).
7. Gungor, C. *et al.* Proteasomal selection of multiprotein complexes recruited by LIM homeodomain transcription factors. *Proc. Natl Acad. Sci. USA* **104**, 15000–15005 (2007).
8. Johnsen, S. A. *et al.* Regulation of estrogen-dependent transcription by the LIM cofactors CLIM and RLIM in breast cancer. *Cancer Res.* **69**, 128–136 (2009).
9. Ostendorff, H. P. *et al.* Functional characterization of the gene encoding RLIM, the corepressor of LIM homeodomain factors. *Genomics* **69**, 120–130 (2000).
10. Ostendorff, H. P. *et al.* Dynamic expression of LIM cofactors in the developing mouse neural tube. *Dev. Dyn.* **235**, 786–791 (2006).
11. Wagner, K. U. *et al.* Spatial and temporal expression of the Cre gene under the control of the MMTV-LTR in different lines of transgenic mice. *Transgenic Res.* **10**, 545–553 (2001).
12. Soriano, P. Generalized lacZ expression with the ROSA26 Cre reporter strain. *Nature Genet.* **21**, 70–71 (1999).
13. Oshima, R. G., Howe, W. E., Klier, F. G., Adamson, E. D. & Shevinsky, L. H. Intermediate filament protein synthesis in preimplantation murine embryos. *Dev. Biol.* **99**, 447–455 (1983).
14. Feinberg, R. F. *et al.* Plasminogen activator inhibitor types 1 and 2 in human trophoblasts. PAI-1 is an immunocytochemical marker of invading trophoblasts. *Lab. Invest.* **61**, 20–26 (1989).
15. Beck, F., Erler, T., Russell, A. & James, R. Expression of Cdx-2 in the mouse embryo and placenta: possible role in patterning of the extra-embryonic membranes. *Dev. Dyn.* **204**, 219–227 (1995).
16. Marahrens, Y., Panning, B., Dausman, J., Strauss, W. & Jaenisch, R. Xist-deficient mice are defective in dosage compensation but not spermatogenesis. *Genes Dev.* **11**, 156–166 (1997).
17. Plath, K. *et al.* Role of histone H3 lysine 27 methylation in X inactivation. *Science* **300**, 131–135 (2003).
18. Barlow, P. W. & Sherman, M. I. The biochemistry of differentiation of mouse trophoblast: studies on polyploidy. *J. Embryol. Exp. Morphol.* **27**, 447–465 (1972).
19. Stavropoulos, N., Lu, N. & Lee, J. T. A functional role for *Tsix* transcription in blocking *Xist* RNA accumulation but not in X-chromosome choice. *Proc. Natl Acad. Sci. USA* **98**, 10232–10237 (2001).
20. Lee, J. T. Disruption of imprinted X inactivation by parent-of-origin effects at *Tsix*. *Cell* **103**, 17–27 (2000).
21. Hall, L. L. *et al.* An ectopic human XIST gene can induce chromosome inactivation in postdifferentiation human HT-1080 cells. *Proc. Natl Acad. Sci. USA* **99**, 8677–8682 (2002).
22. Okamoto, I., Otte, A. P., Allis, C. D., Reinberg, D. & Heard, E. Epigenetic dynamics of imprinted X inactivation during early mouse development. *Science* **303**, 644–649 (2004).
23. Sun, B. K., Deaton, A. M. & Lee, J. T. A transient heterochromatic state in *Xist* preempts X inactivation choice without RNA stabilization. *Mol. Cell* **21**, 617–628 (2006).
24. Jonkers, I. *et al.* RNF12 is an X-encoded dose-dependent activator of X chromosome inactivation. *Cell* **139**, 999–1011 (2009).
25. Nusslein-Volhard, C., Frohnhofer, H. G. & Lehmann, R. Determination of anteroposterior polarity in *Drosophila*. *Science* **238**, 1675–1681 (1987).
26. Letterio, J. J. *et al.* Maternal rescue of transforming growth factor- β 1 null mice. *Science* **264**, 1936–1938 (1994).
27. Guidi, C. J. *et al.* Disruption of *Ini1* leads to peri-implantation lethality and tumorigenesis in mice. *Mol. Cell. Biol.* **21**, 3598–3603 (2001).
28. Tursun, B. *et al.* The ubiquitin ligase Rnf6 regulates local LIM kinase 1 levels in axonal growth cones. *Genes Dev.* **19**, 2307–2319 (2005).
29. Chung, Y. *et al.* Embryonic and extraembryonic stem cell lines derived from single mouse blastomeres. *Nature* **439**, 216–219 (2006).

Supplementary Information is linked to the online version of the paper at www.nature.com/nature.

Acknowledgements We thank V. Boyartchuk, T. Fazio, E. Heard, P. Kaufman, O. Rando, D. Riethmacher and J. Sharp for advice and/or reagents, D. Kim for help in ES cell analysis, and J. Zhu for statistics. I.B. is a member of the University of Massachusetts DERC (DK32520). This work was supported by National Institutes of Health grants R01CA131158 (National Cancer Institute) and 5 P30 DK32520 (National Institute of Diabetes and Digestive and Kidney Diseases) to I.B., and GM053234 to J.B.L.

Author Contributions J.S. and I.B. conceived and designed the experiments. M.B., I.H.-B. and I.B. generated the floxed *Rnf12* mice. J.S. and Y.C. established and analysed ES cell lines. J.S., M.B., H.M., M.B., N.T.-I., X.Z. and B.J. performed experiments. All authors analysed the data. I.B. wrote the manuscript.

Author Information Reprints and permissions information is available at www.nature.com/reprints. The authors declare no competing financial interests. Readers are welcome to comment on the online version of this article at www.nature.com/nature. Correspondence and requests for materials should be addressed to I.B. (ingolf.bach@umassmed.edu).

METHODS

Mice. The targeting vector for the generation of conditional *Rnf12* knockout mice was constructed by inserting three genomic fragments (5.5, 3.3 and 2.7 kb in length) spanning exons 3, 4 and 5 of the *Rnf12* gene⁹ into the basic vector pTV Flox-O (gift from D. Riethmacher) containing a thymidine kinase gene as a negative selection marker. Exon 5 was flanked by *loxP* sites by the insertion of a single *loxP* site into intronic sequences between exons 4 and 5 into a basic vector *AscI* restriction site and by the insertion of a floxed neomycin resistance (*neo*) cassette into the 3' untranslated region of exon 5 with the use of *PmlI* and *NotI* restriction sites. The linearized construct was electroporated into R1 ES cells (derived from strain 129). G418-resistant clones were analysed by Southern blotting with *AvalI*/*AscI* and *AvalI/XhoI* (*AvalI*) and external probes. Correctly targeted ES cells were transfected with a Cre-recombinase-expressing plasmid (gift from D. Riethmacher) to remove the neomycin cassette and analysed by PCR. Two independent ES cell clones were used for the generation of the conditional *Rnf12* knockout line. The ES cells were injected into C57BL/6 blastocysts to generate male chimaeras that were backcrossed with C57BL/6 females. Heterozygous animals derived from two different ES-cell clones were inbred to yield mutant mouse lines. Genotypes were determined by PCR on tail biopsy DNA. To distinguish *MMTV-Cre*-positive $\Delta m/fll$ from *fll/fll* female offspring in some matings, we verified genotypes on genomic DNA collected from liver samples in which Cre-mediated recombination rates were low. For PCR genotyping, the sense primer Kontrolle-newkKO-5'-3' (5'-GGA AATGCTGTGTTGATGCCCGC-3') and the antisense primers ploxP-DR-16-5'c (5'-GTGGCGCGCCGGCTGCAGGAATTCGATATC-3') and Kontrolle-newkKO-Asc-neg (5'-CCTGCAGAGAAGCACCATTTTC-3') were used in a single mix. The primer pair Kontrolle-newkKO-5'-3'/ploxP-DR-16-5'c amplified a 233-bp floxed allele, and the primer pair Kontrolle-newkKO-5'-3'/Kontrolle-newkKO-Asc-neg amplified a 157-bp WT allele. To identify the recombined allele, primer Kontrolle-newkKO-3'-5' (5'-CAGAATGTGAACGAATTTGTGTC-3') was added to the Kontrolle-newkKO-5'-3'/Kontrolle-newkKO-Asc-neg primer mixture, thus amplifying a 291-bp knockout allele in addition to the 157-bp WT allele.

Transgenic *MMTV-Cre* (Line F) mice (B6.Cg-Tg(MMTV-Cre)22Mam) that express Cre recombinase under the control of the *MMTV-LTR*³⁰ were obtained from the MMHCC repository (NCI). Transgenic *MMTV-Cre* (Line D) mice³⁰ and *Rosa26LacZ* mice¹² were purchased from the Jackson Laboratory (B6129-tg(MMTV-Cre)4Mam and B6.129S4-Gt(ROSA)26Sor^{tm1.50r/J}, respectively). All mice were kept in a C57/B6 congenic background and bred in the UMMS animal facility in accordance with National Institutes of Health guidelines, established by the Institute of Animal Care and Usage Committee.

Antibodies and Immunodetections. Antibodies against the following were used: rabbit RLIM, CLIM⁶, guinea pig RLIM¹⁰, glyceraldehyde-3-phosphate dehydrogenase (Chemicon), Cre (Covance), Myc (Abcam), Cdx2 (BioGenex), TATA-box-binding protein (TBP; Millipore), PAI-1 (sc-8979; Santa Cruz), Id1 (sc-488; Santa Cruz), histone H3K27me3 (Abcam), β -Gal (Abcam), and Oct4 and Nanog (Bethyl Laboratories). Antibodies against SSEA-1 and Troma-1 were obtained from the Developmental Studies Hybridoma Bank developed under the auspices of the National Institute of Child Health and Human Development and maintained by The University of Iowa. Immunocytochemistry and western blots were performed as reported previously^{28,29}. Placentae and ovaries were fixed in 4% paraformaldehyde, and paraffin-embedded sections were stained with H&E (Histoserv, Inc.). Immunohistochemical stainings of paraffin sections were performed in the DERC Morphology Core facility at UMMS.

ES cells. Wild-type mouse female ES cells (ES2-1 line)¹⁶ were obtained from the Panning laboratory (gift from J. Sharp). ES cells were cultured in DMEM medium containing 15% FBS, penicillin/streptomycin, 2 mM L-glutamine, 1 mM 2-mercaptoethanol, 1 mM sodium pyruvate (Gibco) and 1000 U ml⁻¹ mouse leukaemia inhibitory factor (LIF; Chemicon). For differentiation, 10⁵ cells were cultured in bacterial Petri dishes in the absence of LIF for 2 days³¹.

Generation and analysis of ES cells mutated in *Rnf12*. Procedures used for the derivation of mouse ES cells have been described previously³². In brief, 5 U of pregnant mare serum gonadotropin (Calbiochem) and 5 U of human chorionic gonadotropin (hCG; Sigma-Aldrich) were used to induce superovulation in 8–10-week-old female *fll*/ Δp mice. Immediately after hCG injection, mice were mated with Δ/Y males to obtain fertilized embryos. At 48 h after hCG injection, eight-cell stage embryos were flushed from the oviduct and cultured in KSOM medium (Specialty Media) until they developed to an expanded blastocyst stage. To facilitate their attachment to MEFs, the zona pellucida of blastocysts were removed by brief exposure to acidic Tyrode solution (Specialty Media) and denuded embryos were plated onto MEFs prepared in four-well dishes. The ES-cell derivation medium was composed of 2,000 U ml⁻¹ mouse leukaemia inhibitory factor (LIF; Chemicon) and 50 μ M MEK1 inhibitor (Cell Signaling Technology) in knockout DMEM (Gibco) supplemented with glutamine, MEM non-essential amino acids, 2-mercaptoethanol, antibiotics (Gibco) and 20% fetal

calf serum (Hyclone). About 3 days after plating, the initial outgrowth of inner cell mass was mechanically disrupted and transferred to a fresh culture dish. After three more mechanical passages, the newly established ES cell lines were expanded by treatment with 0.05% trypsin-EDTA (Invitrogen). ES cells were tested for expression of ES-cell markers Oct4, Nanog, AP and SSEA1 and karyotyped by Cell Line Genetics. The teratoma analyses of Δ/Δ ES cells were performed as described previously³³. In brief, 50–100 cells were injected under the kidney capsule of 6–8-week-old NOD-SCID male mice (Jackson Laboratories). After a further 7–12 weeks, mice were killed and the kidneys were fixed in 4% paraformaldehyde. Paraffin-embedded sections were stained with H&E.

Preparation of early embryos, blastocyst outgrowths and RT-PCR. To obtain blastocysts and early embryos, 8–14-week-old female mice were naturally mated with males. Early embryos were collected at the two-cell, four-cell and eight-cell stage and adhered to coverslips coated with Cell-Tak (BD Biosciences). Blastocysts were collected at E3.5 or E4.5 and cultured for 2–3 days on gelatin-coated coverslips until trophoblasts formed a monolayer away from the ICM, as described previously^{27,34}. For genotyping of blastocysts, primers used to detect the *Zfy* gene were *Zfy1* (5'-GATAAGCTTACATAATCACATGGA-3') and *Zfy2* (5'- CCTAT GAAATCCTTTGCTGC-3'). Primers used to amplify the β -actin gene were *Act1* (5'-GCAAGTGCTCTAGGCGGAC-3') and *Act2* (5'-AAGAAAGGGTGTAAACGCAGC-3'). RNA isolation for RT-qPCR was performed using a Dynabeads mRNA DIRECT Kit (Invitrogen) in accordance with the manufacturer's instruction. Sex identification was performed by semiquantitative RT-PCR with a OneStep RT-PCR Kit (Qiagen). Real-time PCR on female blastocysts was performed with a Power SYBR Green PCR Master Mix (Applied Biosystems). The amplification condition was as follows: initial denaturation for 2 min at 94 °C and 40 cycles of 40 s at 94 °C, annealing for 30 s at 60 °C and elongation for 40 s at 72 °C. Primers were *Xist1* (5'-GCCAACCAATGAGACCACCT-3'), *Xist2* (5'-TTCTCTCAAACCACACACG-3'), *Tsix1* (5'-TACCTGCAAGCGCTACACAC-3'), *Tsix2* (5'-GCTGGCTATACGCTCTCT-3'), *PGK1* (5'-GACTTAGGAGCACAGGAACC-3') and *PGK2* (5'-GACTTAGGAGCACAGGAACC-3')³⁵. β -Actin was used as the internal control to normalize individual amplifications. RT-PCR on ES cells was performed with a OneStep RT-PCR Kit (Qiagen). Primers were *Rlim* Exon24RT-F (5'-CCAGCAAATGTTGTCTCTC-3'), *Rlim* Exon24RT-R (5'-CCGAAACACCGTGTAAAGTGA-3'), *Rlim* Exon5RT-F (5'-GCAAGGTAGTTACGAAGTT-3'), *Rlim* Exon5RT-R (5'-TCCGAGAGTAGCTCAGAGAT-3'), *Beta* Actin F (5'-TTCCGATGCCCTGAGGCTCT-3') and *Beta* Actin R (5'-TGCTGATCCACATCTGCTGG-3').

RNA FISH. Hybridization to RNA was performed as described or in accordance with the manufacturer's directions (Qbiogene). DNA probes were nick-translated with either biotin-11-dUTP or digoxigenin-16-dUTP (Roche Diagnostics). RNA-specific hybridization was performed under non-denaturing conditions where the DNA was not accessible. In brief, RNA was hybridized overnight at 37 °C, in 2 \times SSC, 1 U μ l⁻¹ RNasin and 50% formamide, with 2.5 μ g ml⁻¹ DNA probe. Cells were washed for 20 min in 50% formamide/2 \times SSC at 37 °C, for 20 min in 2 \times SSC at 37 °C; for 20 min in 1 \times SSC at room temperature (25 °C), and for 5 min in 4 \times SSC at room temperature. Detection was performed for 1 h with anti-digoxigenin bound to rhodamine (200 μ g ml⁻¹) or fluorescein-conjugated avidin (2.5 mg ml⁻¹) in 1% BSA/4 \times SSC at 37 °C. Post-detection washes were performed sequentially with 4 \times SSC, with 4 \times SSC containing 0.1% Triton, and with 4 \times SSC, each for 10 min at room temperature, in the dark. Templates for the synthesis of specific probes were plasmids containing mouse *Xist* exon 1 and 6 that recognizes *Xist* and *Tsix*³⁶. For *Pgk1*, plasmids were used that contain the entire coding sequence (purchased from Open Biosystems). For *Rnf12* we used a 12-kb genomic probe derived from phage G12 (ref. 9) that contains exon 1, intron 1, exon 2 and most of intron 2. As in the conditional *Rnf12* knockout, exon 5 is flanked by *loxP* sites; this probe detects *Rnf12* RNAs transcribed from both wild-type and knockout alleles. *Cot-1* DNA was purchased from Gibco BRL. The three-dimensional analysis on roughly 60 separate images (0.10- μ m spacing) of WT and Δ/Δ blastocysts at E4.5 stained with a *Xist* probe was performed as described previously³⁷. The deconvolved and reconstructed image stack represents a movie focusing through the ICM.

- Wagner, K. U. *et al.* Cre-mediated gene deletion in the mammary gland. *Nucleic Acids Res.* **25**, 4323–4330 (1997).
- Novik, E. I., Maguire, T. J., Orlova, K., Schloss, R. S. & Yarmush, M. L. Embryoid body-mediated differentiation of mouse embryonic stem cells along a hepatocyte lineage: insights from gene expression profiles. *Tissue Eng.* **12**, 1515–1525 (2006).
- Chung, Y. & Becker, S. Embryonic stem cells using nuclear transfer. *Methods Enzymol.* **418**, 135–147 (2006).
- Chung, Y. *et al.* Human embryonic stem cell lines generated without embryo destruction. *Cell Stem Cell* **2**, 113–117 (2008).
- Nagy, A., Gerstenstein, M., Vintersten, K. & Behringer, R. *Manipulating the Mouse Embryo* (Cold Spring Harbor Laboratory Press, 2003).

35. Marks, H. *et al.* High-resolution analysis of epigenetic changes associated with X inactivation. *Genome Res.* **19**, 1361–1373 (2009).
36. Panning, B. X inactivation in mouse ES cells: histone modifications and FISH. *Methods Enzymol.* **376**, 419–428 (2004).
37. Clemson, C. M., Hall, L. L., Byron, M., McNeil, J. & Lawrence, J. B. The X chromosome is organized into a gene-rich outer rim and an internal core containing silenced nongenic sequences. *Proc. Natl Acad. Sci. USA* **103**, 7688–7693 (2006).